

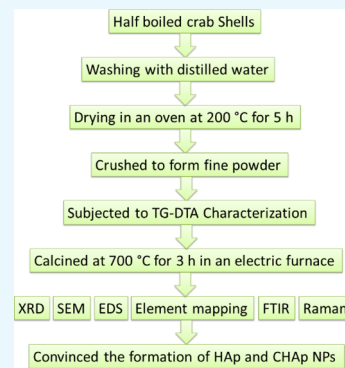
Structure of Apatite Nanoparticles Derived from Marine Animal (Crab) Shells: An Environment-Friendly and Cost-Effective Novel Approach to Recycle Seafood Waste

Birendra Nath Bhattacharjee,[†] Vijay Kumar Mishra,^{*,†,‡} Shyam Bahadur Rai,^{*,‡} Om Parkash,[†] and Devendra Kumar^{*,†}

[†]Department of Ceramic Engineering, Indian Institute of Technology (Banaras Hindu University), Varanasi 221005, Uttar Pradesh, India

[‡]Department of Physics, Institute of Science, Banaras Hindu University, Varanasi 221005, Uttar Pradesh, India

ABSTRACT: In the present investigation, crab shells as seafood wastes were successfully recycled into an extremely useful biomaterial by the thermal treatment method. Thermogravimetric-differential thermal analysis studies concluded that the calcination temperature must be beyond ~ 570 °C to get a fine and crystalline apatite powder from the crab shells. Thus, the calcination temperature is taken to be 700 °C. Powder X-ray diffraction analysis of the calcined crab shells revealed hydroxyapatite (HAp)/carbonated HAp (CHAp) with an average crystallite size of 24.4 nm. Scanning electron microscopy revealed the surface morphology of the crab shells-derived apatite powder as needle-like nanorods of HAp of diameter ≈ 100 –300 nm and nanospheres of CHAp of diameter ≈ 100 –500. Energy-dispersive X-ray spectroscopy showed the presence of calcium, phosphorous, magnesium, and oxygen as major elements in the apatite constituents. Fourier transform infrared as well as Raman spectroscopies confirmed the formation of apatite powder. X-ray photoelectron spectroscopy results indicated the electronic environment and oxidation states of the constituent elements, Ca, C, and P. On the basis of the results obtained from various characterization techniques, the overall study emphasized an environment-friendly and cost-effective approach for recycling of the bio-pollutant and synthesis of ultra-fine, ultra-crystalline apatite-based excellent biomaterial derived from crab shells as seafood wastes with its application as a futuristic biomaterial in bone/teeth implants.



INTRODUCTION

Seafood processing produces a very large quantity of solid and liquid wastes. There is a large demand of an effective strategy for the utilization that can minimize the environmental pollution by recovering the products of commercial interest from the industry waste obtained during seafood processing. Biomaterials derived from biological wastes (taken as resources) are generally abundant, renewable, inexpensive, and environment-friendly as compared to artificial biomaterials synthesized chemically. Seafood and other value-added goods obtained during processing have a marketable demand. In the past 20 years, the business in this area have grown to become a billion-dollar industry.¹ The rising demand of such products has resulted in the growth of fishing and aquaculture business across the world. The highly consumable seafood, needs to be processed to extend its shelf-life. Similar to most of the food industries, fish processing also produces waste (fish carcasses, viscera, skin, and heads). If 45% of the live weight is considered as waste material, then nearly 63.6 million metric tons of waste would be generated globally.² Therefore, aquaculture and the food-processing industries produce a huge quantity of waste globally each year. Hence, solid wastes generated on a huge scale by the seafood industries and its removal has become a horrific trouble nowadays. An attractive management of such

waste produced from seafood processing is urgently required because it is a major cause for the environmental problems associated with discarding it in the ocean, dumping on the land, which again raise problems related to unnecessary nutrient inputs.³ It is noteworthy to mention that the disposal of seafood waste is very costly due to firm environmental regulations.⁴ Therefore in current situation one of the instant solutions for this issue is to utilize/recycle the waste materials in such such a way that it can be cost-effectively and resourcefully used to produce other useful materials and products which may additionally resolve some financial problems of purchasing of costly materials.⁵

Crab shells are the most common and chief waste produced by the seafood industry. Many successful methods were adopted for the utilization of crab shells in different applications such as a source of chitin, metal removal from aqueous solutions, and in drug delivery systems.^{6–9} A novel and potential application of crab shells as seafood waste is strongly anticipated in the production of some extremely important calcium phosphate biomaterials/apatite/hydroxya-

Received: January 15, 2019

Accepted: July 12, 2019

Published: July 26, 2019

apatite (HAp)/carbonated HAp (CHAp) powders similar to the production of apatite powders from bovine, sheep and goat, skeletons, as crab shells also mainly contain the carbonates of calcium and magnesium.¹⁰ HAp, $\text{Ca}_{10}(\text{PO}_4)_6(\text{OH})_2$, is chemically similar to the mineral component of mammals bones, and hence has the ability to interact with bones.¹⁰ Therefore, research on HAp has been progressing exponentially to seek the possibilities of use of HAp as a bone replacement material.¹⁰ Concurrently, researchers are also using various procedures for the improvement of mechanical, biocompatibility, and electrical properties of thus-prepared biological HAp.^{11,12} HAp promotes bone ingrowths when used in orthopedic, prosthetic, and dental implant applications.¹³ HAp with stoichiometric composition and Ca/P(ratio) = 1.67 has generated much awareness in the context of bone and teeth implants due to its resemblance with the mineral constituent of mammalian bones and teeth. Conversely, HAp may be produced from mammalian bones. By using this idea worldwide, a large number of industries are working for apatite products from biological resources, particularly from bovine bones supplied from slaughterhouse/meat packaging industries. Therefore, the research on seeking different possibilities and methods of recycling the waste material/bio-pollutants into useful product(s) is quite necessary because these methods will, on one hand, minimize the danger of diseases rising due to air and water pollution caused by dumping of wastes and prevent polluting the environment and fouling the earth. Moreover, the recycling of the seafood waste/bio-pollutants may offer industry-level production of extremely important materials/biomaterials, on the other hand. However, somehow, recycling of crab shells could not be yet attempted unlike the recycling of skeletons of bovine and other mammals. The main reason behind this was the lack of proper information about the structure and biological behavior of the thermally processed powder of crab shells. Therefore, utilization of the processed powder could not be determined. This motivated us to investigate the structure and biological behavior of thermally processed crab shell powders to establish the recycling of crab shell-like seafood waste into a biomaterial, which may have extreme potential as a xenograft material and that will consequently promote-cum-offer the production of biomaterials from crab shells on an industrial level. Therefore, comprehensive investigations on structural analysis, *in vitro* cytotoxicity, and bone-forming efficacy of the crab shell-derived apatite powder are urgently required. The present work provides the demonstrated solid model to save the environment and the planet we live on. Our study creates a paradigm for future studies, specifically *in vitro* and *in vivo* applications.

The heat treatment method of extracting HAp from crab shells is adopted in the present investigation because it is a simple, economical, quick, and appropriate approach. It involves a solid-state reaction route and does not involve the presence of impurities, which appear because of the use of solvents, acids, microbes, and so forth. In addition to this, the solid-state reaction route is the most widely used method for the preparation of polycrystalline nano-HAp from biological resources.¹⁴ Solids do not react together at room temperature and a much higher temperature is required for that. During the heat treatment of biological samples, there is combustion of organic substances contained in the form of proteins and collagens get volatilized and removed.¹⁵ In the present investigation, half-boiled crab shells were washed and dried,

and thereafter, the dried sample was subjected to thermal treatment. The thus-obtained calcined powder of crab shells was further characterized to determine the crystal structure, microstructure, and molecular structure, of the calcined powder of crab shells to determine its possible application as a futuristic biomaterial in bone/teeth implants, tissue engineering, and drug delivery.

■ EXPERIMENTAL SECTION

Materials and Methods. Half-boiled crab shells treated as waste were collected from the fishermen residing in areas of the Puri sea beach, Odisha, India. The crab shells as obtained in the original form were thoroughly washed with triply distilled water and were dried in an oven at 200 °C for 5 h. The dried crab shells were crushed to form crab shell powder by using mortar and pestle. The crab shell powder was then characterized by thermogravimetric-differential thermal analysis (TG-DTA) to determine the calcination temperature and then calcined in an alumina crucible at 700 °C for 3 h at a heating rate of 5 °C min⁻¹.

Characterization. The thermal behavior of the dried and crushed crab shells is analyzed employing thermogravimetric analysis (TGA) and DTA by using a TG-DTA model no. Labsys 16, Setaram by heating the samples up to 600 °C in air at the heating rate of 10 °C min⁻¹. The dried and crushed crab shells were calcined at 700 °C in air at a heating rate of 5 °C min⁻¹ for 3 h. The calcined sample is characterized for the determination of crystal structure and phase constitution using X-ray diffraction (XRD) by using a Rigaku Desktop Miniflex II X-ray diffractometer, Tokyo, Japan, equipped with Cu K α radiation as the source of X-ray and a nickel filter. The molecular structure of the sample is analyzed using Fourier transform infrared (FTIR) spectroscopy by using a PerkinElmer spectrum 65, FTIR spectrometer, MA using KBr pellet with the calcined sample in the ratio KBr/sample: 1:10. The calcined sample is also studied by Raman spectroscopy to investigate the nature of chemical functional groups present in it using a micro-Raman setup, Renishaw (Gloucestershire, UK) having grating of 1800 lines mm⁻¹ and a Peltier cooled CCD. A microscope from Olympus, model number MX50A/T, Olympus, Hamburg, Germany is attached to the spectrometer to focus the laser light onto the sample and collect the scattered light at 180° scattering geometry. The 514.5 nm line of Ar⁺ laser is used as the excitation source, and the GRAM-32 (Adent Scientific plc., Hertfordshire, UK) software is used for data collection. The microstructure of the calcined sample is studied by using scanning electron microscopy (SEM) on applying an extra high tension of 20 kV to the metal-coated powder samples using Inspect S-50, FEI Company of USA (SEA) PTE Ltd., Singapore, FP 2017/12 scanning electron microscope. Energy dispersive X-ray spectroscopy (EDS) of the calcined sample is also performed to analyze the elements present in the calcined sample. In order to study the electronic environment and chemical oxidation states of the elements present in the samples, X-ray photoelectron spectroscopy (XPS) is carried out using Amicus, Kratos Analytical (Shimadzu), Spectroscopy. The binding energy in XPS analysis is corrected by the C (1s) adventitious peak.

■ RESULTS AND DISCUSSION

Thermal Analysis. The thermal behavior of the dried and crushed crab shells is studied by heating the sample from room

temperature up to 600 °C by using TG-DTA (Figure 1). The TGA curve is divided into segments depending on the

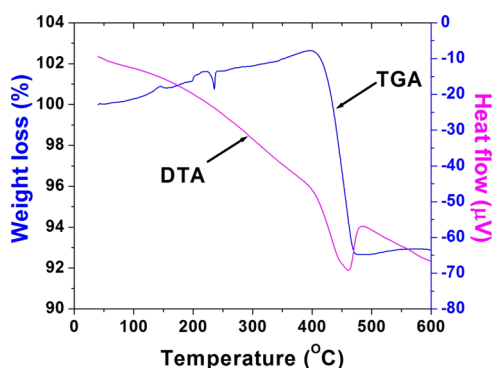


Figure 1. TG-DTA of the dried crab shells before heat treatment (calcinations). The havoc weight loss is due to the removal of the organic part, that is, collagen from the crab shells and formation of apatite nodules.

temperature range; room temperature –400, 400–470, and 470–600 °C. Initially, in the first segment (room temperature –400 °C), a weight gain of ~3% of total weight is observed that may be attributed to the presence of something in the system which is oxidizing and resulting in the gain in mass. In the second segment (400–470 °C), the sample exhibited the total weight loss of ~7% of initial weight as followed by an endothermic peak-cum-envelope at ~460 °C in the DTA curve, which clearly indicates the removal of absorbed water, organic ingredients (collagen) of crab shells, and other biological compounds. This DTA peak is observed to be wide like an envelope rather than a sharp one showing regular heat flow (i.e., continuous endothermic nature) from the very beginning (room temperature –400 °C) because of the presence of absorbed water and other biological compounds; however, the second segment of this envelope (400–460 °C) was comparatively sharper than the previous and is attributed to the presence of CHAp and other minerals in crab shells as biological apatite contains type-B CHAp. In the third segment (470–600 °C), no significant weight loss is observed; however, the DTA curve shows an exothermic peak at ~480 °C that may be due to the formation of biological HAp nodules. However, crystallization temperature of type-B CHAp may be different, hopefully more than the crystallization temperature of HAp and could be obtained by heating this sample up to 1000 °C. TG-DTA studies finally gave the idea of the calcination temperature to which the crab shell powder must be heated for the formation of the apatite nodules as a true biomaterial. The calcination temperature for crab shell powder is therefore taken as 700 °C for the sample in bulk amount. This temperature should be enough to remove the organic part of the crab shells/bones present in the form of extra cellular matrix containing collagen fibers.

Crystal Structure. The crystal structure of the calcined sample is studied by using XRD as given in Figure 2 and a careful comparison of the XRD pattern with the JCPDS (file no. 24-0033) for hexagonal HAp indicated that all of the diffraction peaks of the sample are in good agreement with the standard data for HAp and CHAp. All high intensity peaks in the XRD pattern revealed that the HAp appeared in major form in the calcined crab shells. However, three peaks due to planes *(210) at 29°, *(302) at 43°, and *(132) at 47°

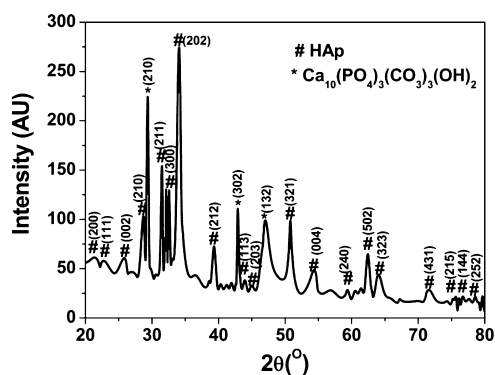


Figure 2. XRD pattern of crab shells powder calcined at 700 °C for 3 h. XRD revealed that the calcined crab shells powder is nothing but a specific mixture of HAp and CHAp as the characteristic parts of the biological apatite.

revealed the presence of CHAp ($\text{Ca}_{10}(\text{PO}_4)_3(\text{CO}_3)_3(\text{OH})_2$) with JCPDS file no. 19-0272 in the crab skeleton, which is the characteristic part of the biological apatite. On refinement using Unit Cell Software,¹⁶ it was observed that the lattice parameters and volume of the calcined crab shells were in close agreement with that of HAp and CHAp as given in Table 1. The average crystallite size of the calcined crab shells is calculated using the Scherer's formula which is given by

$$D = \frac{0.9\lambda}{\beta \cos \theta} \quad (1)$$

where D is the crystallite size, λ is the wavelength which is equal to 1.5406 Å, β is the full width at half-maximum (fwhm) in radians, and θ is the diffracted angle. The average crystallite size is found to be 24.4 nm. The fine and sharp peaks observed in the XRD pattern also suggest high crystallinity of the calcined crab shells.

Microstructure Analysis. The SEM image of the crab shells calcined at 700 °C is shown in Figure 3. The SEM image is taken at magnification of 20 000×. The overall morphology clearly indicates that some rod-like nanostructures with diameter around 100–300 nm and length around 600 nm are present. SEM results revealed that nanorods of HAp are present in the skeletons of crabs (phylum: euarthropoda, class: malacostraca), mammals, few birds, and other sea animals. Most of the birds and reptiles are to be investigated in the aspect of the morphology/histology of their skeletons. Hexagonal HAp has an intrinsic (002) face preference for growth, which always facilitates the formation of rods rather than particles.¹⁷

Figure 4a–f depicts (a) EDS pattern and mapping of the elements (b) calcium, (c) chlorine, (d) phosphorous, (e) magnesium, and (f) oxygen as their distribution on the surface of the calcined crab shells sample. EDS of the calcined sample indicates the presence of calcium, magnesium, chlorine, oxygen, and phosphorous with atomic % of 30.18, 2.44, 1.85, 55.94, and 9.59, respectively. Calcium, magnesium, phosphorous, and oxygen were distributed in higher amounts as compared to chlorine. Conversely, it is observed that chlorine is very less dense and pertains to the surface only as compared to calcium, phosphorous, magnesium, and oxygen.

Molecular Structure. Figure 5 depicts the FTIR and Raman spectrum of the calcined crab shells sample. Both the spectra were recorded in the wavenumber range 4000–400 cm^{-1} . All absorption peaks in the FTIR spectrum and

Table 1. Lattice Parameters and Volume of the Phases of HAp, CHAp, and Crab Shells Powder Calcined at 700 °C

compound	chemical formula	space group	lattice parameters		volume (cm ³)
			<i>a</i> = <i>b</i>	<i>c</i>	
hydroxyapatite	Ca ₅ (PO ₄) ₃ (OH)	<i>P</i> 6 ₃ / <i>m</i>	9.432	6.881	530.13
carbonated hydroxyapatite	Ca ₁₀ (PO ₄) ₃ (CO ₃) ₃ (OH) ₂	<i>P</i> 6 ₃ / <i>m</i>	9.309	6.927	519.85
crab shells powder calcined at 700 °C			9.456	6.854	530.85

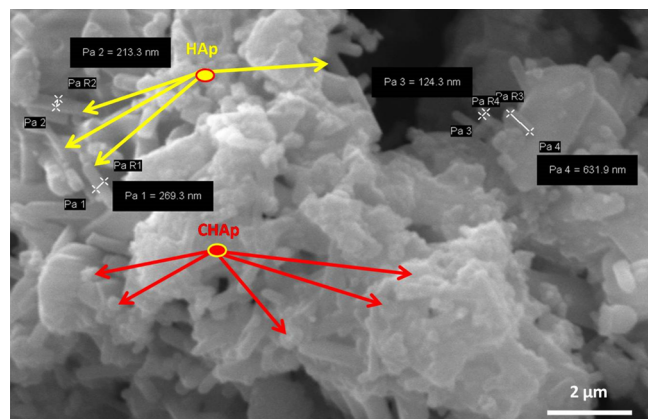


Figure 3. SEM image of calcined crab shells. Image shows that the biological apatite derived from crabs have nanorods of HAp of dimensions ~ 200 nm \times 600 nm along with the carbonated (HAp). Yellow-colored arrows indicate the nanorods of well crystallized HAp; however, red-colored arrows show the crystallized nanospheres as well as semicrystallized undeveloped grains of CHAp. Complete crystallization of CHAp needs comparatively slow heating rate and more holding time for calcination as compared to pure HAp.

scattering peaks in the Raman spectrum along with their assignments are enlisted in Table 2. A careful examination of the FTIR spectrum of the calcined powder reveals that all observed bands may be attributed to one or the other vibrational mode of pure HAp. It is totally pertinent to note herein that totally symmetric modes have a higher intensity in the Raman spectrum, whereas the corresponding IR bands have lower intensity for symmetric modes in IR. Reverse is the case for asymmetrical modes in IR and the Raman spectrum. The lowest wavenumber peak in IR is observed at 563 cm⁻¹ which is due to the ν_4 bending mode of O–P–O. Also, the

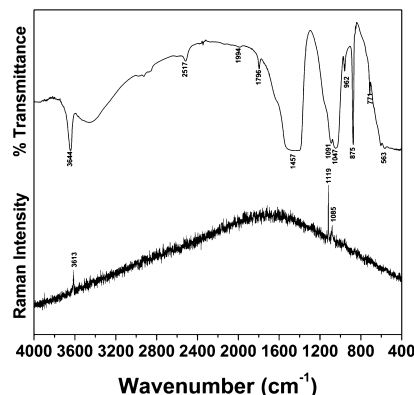


Figure 5. FTIR spectrum of calcined crab shells in the upper panel and Raman spectrum of calcined crab shells in the lower panel. Both the spectra jointly convinced that calcined crab shells are nothing but HAp/CHAp.

peak at 771 cm⁻¹ is due to the Ca(OH)₂ vibration band. The presence of carbonate ions (CO₃²⁻) is indicated by the peak at 875 cm⁻¹. The ν_1 -symmetric stretching mode of PO₄³⁻ is obtained at 962 cm⁻¹.¹⁸ Absorption peaks at wavenumber 1047 , 1091 , and 1119 cm⁻¹ in the IR spectrum represent the ν_3 P–O asymmetric stretching modes of the orthophosphate groups of the calcined sample.¹⁸ The corresponding band in the Raman spectrum appears at 1085 cm⁻¹. A high intensity absorption band centered at 1457 cm⁻¹ is attributed to the ν_3 -mode of carbonate ions (CO₃²⁻) of type-B CHAp. Three absorption peaks appear at 1796 , 1994 , and 2517 cm⁻¹ and are attributed to the stretching vibrations of carbonate ions (CO₃²⁻) in the IR region. A medium intensity sharp peak at 3644 cm⁻¹ depicts the stretching modes of OH⁻. The similar band in the Raman profile appears at 3613 cm⁻¹. This may be due to the presence of hydrogen-bonded H₂O (see Table 2).

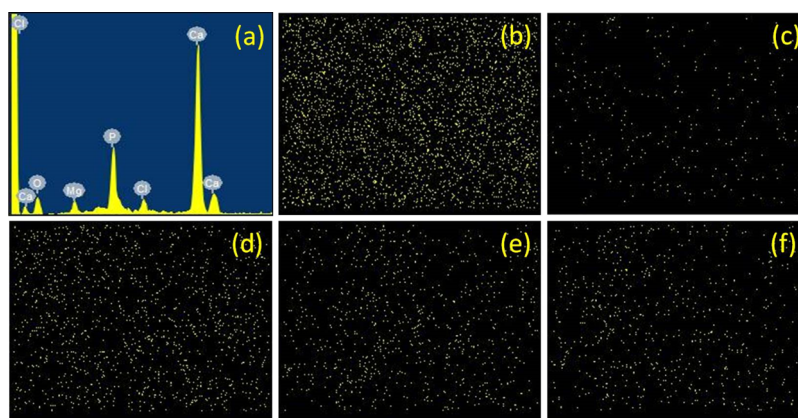


Figure 4. (a–f): (a) EDS pattern and mapping of few elements, (b) calcium, (c) chlorine, (d) phosphorous, (e) magnesium, and (f) oxygen as their distribution on the surface of the calcined crab shells sample. The EDS indicated the presence of calcium, magnesium, chlorine, oxygen, and phosphorous with atomic % of 30.18, 2.44, 1.85, 55.94, and 9.59, respectively. Calcium, magnesium, phosphorous, and oxygen are distributed in more amounts as compared to chlorine. Conversely, chlorine is very less dense and pertains to the surface only.

Table 2. FTIR and Raman Active Vibrational Bands of Crab Shells Powder Calcined at 700 °C and Their Assignments

FTIR (in cm^{-1})	Raman (in cm^{-1})	assignments
563		ν_4 bending mode of O–P–O
771		Ca(OH) ₂ vibration band
875		ν_2 carbonate ions (CO_3^{2-})
962		ν_1 stretching mode of PO_4^{3-}
1047		ν_3 P–O asymmetric stretching
1091	1085	ν_3 P–O asymmetric stretching
	1119	ν_3 P–O asymmetric stretching
1457		ν_3 carbonate ions (CO_3^{2-})
1796		carbonate ions (CO_3^{2-})
1994		carbonate ions (CO_3^{2-})
2517		carbonate ions (CO_3^{2-})
	3613	hydrogen-bonded H ₂ O
3644		stretching mode of the OH ⁻ bands

Spectroscopic characterizations confirm the presence of HAp/CHAp in the calcined crab shells.

XPS of Calcined Crab Shells. XPS analysis is also performed to confirm the presence of constituting elements in the calcined crab shells powder. Existence of an element is detected by the binding energy associated with a particular electronic state of that element. The electronic environment and oxidation states of the elements contained in the calcined crab shells studied using XPS are shown in Figure 6a–d illustrating the XPS profiles of the high-resolution spectra of specific constituent elements of the calcined crab shells sample as (a) full spectrum, (b) calcium element, (c) carbon element, and (d) phosphorous element. The binding energy in the XPS analysis is corrected by the C (1s) adventitious peak. Figure 6a exhibits that calcined crab shells are mainly composed of Ca, C, P, and O. The peak observed at 286 eV is because of C 1s due to the adventitious hydrocarbon from the XPS instrument. The Ca 2p_{1/2} and Ca 2p_{3/2} are found to be located at binding energies of 352 and 348 eV, occupying areas of 3911 and 9134, having fwhm of 1.870 and 2.057 eV, respectively (see Figure

6b). The C is found to be located at two different regions, one indicating C bonded to the carbonate (CO_3^{2-}) group and another due to C 1s peak of binding energies of 291 and 286 eV, respectively (see Figure 6c). The 2p_{3/2} at 133.5 eV and 2p_{1/2} at 134.8 eV indicate the phosphate bonding with calcium in the calcined sample. Like the previous characterization techniques, XPS also confirms the presence of HAp/CHAp in the calcined crab shells.

The above results obtained from different structural, morphological, spectroscopic, chemical, and biological characterization techniques clearly convince that the obtained biological material is the apatite powder of nanostructured HAp/CHAp derived from crab shells. Recent advancements in ceramic fabrication have offered bone reconstruction by choosing a suitable combination of these materials.^{18,19} This method does not require any additional chemicals for the source of calcium, source of phosphorous, capping agent, pH maintaining chemical, such as phosphoric acid or sulfuric compounds, EDTA or CTAB, sodium hydroxide pellets, and so forth that makes its advantages stronger on the environmental benefits and minimizes the cost of the product. Thus, it is worthwhile to state that the employed synthesis method is a very cost-effective and environment-friendly approach for recycling of seafood waste into such an amazing useful apatite nanobiomaterial.

CONCLUSIONS

Apatite NPs of the average crystallite size 24.4 nm and particle size 100–300 nm are successfully derived from crab shells. The obtained powder is the mixture of needle-like nanorods of HAp and nanospheres of CHAp NPs similar to apatite powder derived from other biological sources such as bovine, sheep, human and so forth. The overall study concludes that the present method is an environment-friendly and cost-effective approach to derive apatite powder from crab shells, that has potential applications in bone implants, scaffolds, dentistry, bone cements, tissue engineering, and drug delivery. The crab shells-derived apatite powder is strongly expected to be highly

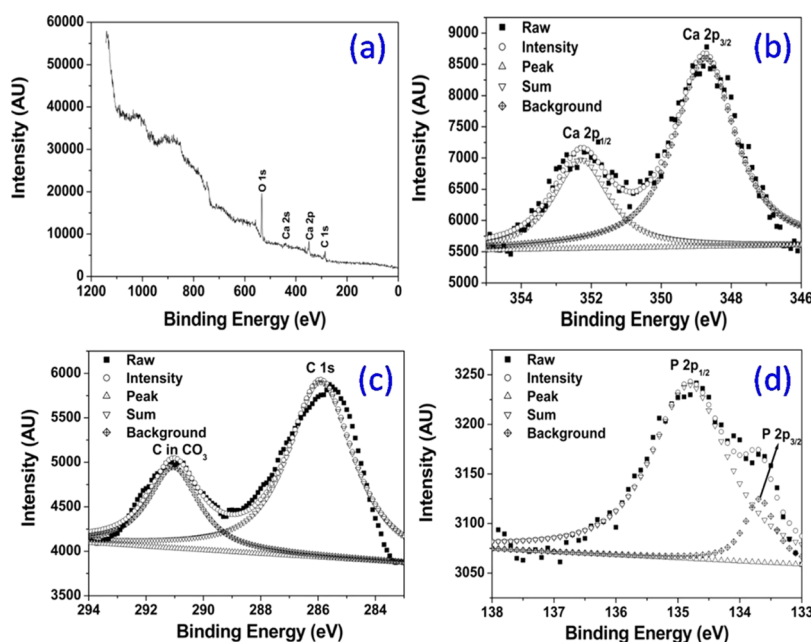


Figure 6. XPS profiles of calcined sample as (a) full spectrum, (b) calcium, (c) carbon, and (d) phosphorous elements.

compatible with osteoblast cells and to have osteogenic behavior as it is the mixture of HAP and CHAp.

AUTHOR INFORMATION

Corresponding Authors

*E-mail: vijaybioceramic@gmail.com (V.K.M.).

*E-mail: sbraibhu@gmail.com (S.B.R.).

*E-mail: devendra.cer@iitbhu.ac.in (D.K.).

ORCID

Vijay Kumar Mishra: 0000-0003-1447-4787

Shyam Bahadur Rai: 0000-0002-6321-1038

Notes

The authors declare no competing financial interest.

ACKNOWLEDGMENTS

The authors would like to express their sincere thanks to Prof. A. S. K. Sinha, Department of Chemical Engineering, Indian Institute of Technology (Banaras Hindu University) for providing the XPS facility. Authors are thankful to Prof. R.K. Singh, Department of Physics, Institute of Science, B.H.U. for the Raman characterization facility. B.N.B. is thankful to the Indian Institute of Technology (B.H.U.) for providing teaching assistantship. V.K.M. acknowledges UGC-RFSMS fellowship (F.5-127/2007 (BSR) 15/03/2013).

REFERENCES

- (1) Alkaya, E.; Demirer, G. N. Minimizing and Adding Value to Seafood Processing Wastes. *Food Bioprod. Process.* **2016**, *100*, 195–202.
- (2) Denham, F. C.; Howieson, J. R.; Solah, V. A.; Biswas, W. K. Environmental Supply Chain Management in the Seafood Industry: Past, Present and Future Approaches. *J. Clean. Prod.* **2015**, *90*, 82–90.
- (3) Dima, J. B.; Sequeiros, C.; Zaritzky, N. E. Hexavalent Chromium Removal in Contaminated Water Using Reticulated Chitosan Micro/Nanoparticles from Seafood Processing Wastes. *Chemosphere* **2015**, *141*, 100–111.
- (4) Esakkiraj, P.; Usha, R.; Palavesam, A.; Immanuel, G. Solid-state Production of Esterase Using Fish Processing Wastes by *Bacillus Altitudinis* AP-MSU. *Food Bioprod. Process.* **2012**, *90*, 370–376.
- (5) Panpong, K.; Srisuwan, G.; O-Thong, S.; Kongjan, P. Anaerobic Co-digestion of Canned Seafood Wastewater with Glycerol Waste for Enhanced Biogas Production. *Energy Procedia* **2014**, *52*, 328–336.
- (6) Monteiro, R. J. R.; Lopes, C. B.; Rocha, L. S.; Coelho, J. P.; Duarte, A. C.; Pereira, E. Sustainable Approach for Recycling Seafood Wastes for the Removal of Priority Hazardous Substances (Hg and Cd) from Water. *J. Environ. Chem. Eng.* **2016**, *4*, 1199–1208.
- (7) Kannan, S.; Garipey, Y.; Raghavan, V. Optimization of Enzyme Hydrolysis of Seafood Waste for Microwave Hydrothermal Carbonization. *Energy Fuels* **2015**, *29*, 8006–8016.
- (8) Vijayaraghavan, K.; Winnie, H. Y. N.; Balasubramanian, R. Biosorption characteristics of crab shell particles for the removal of manganese(II) and zinc(II) from aqueous solutions. *Desalination* **2011**, *266*, 195–200.
- (9) Kusriani, E.; Arbiandi, R.; Sofyan, N.; Abdullah, M. A. A.; Andriani, F. Modification of Chitosan by Using Samarium for Potential Use in Drug Delivery System. *Spectrochim. Acta, Part A* **2014**, *120*, 77–83.
- (10) Lalzawmliana, V.; Anand, A.; Mukherjee, P.; Chaudhuri, S.; Kundu, B.; Nandi, S. K.; Thakur, N. L. Marine organisms as a source of natural matrix for bone tissue engineering. *Ceram. Int.* **2019**, *45*, 1469.
- (11) Gittings, J. P.; Bowen, C. R.; Dent, A. C. E.; Turner, I. G.; Baxter, F. R.; Chaudhuri, J. B. Electrical characterization of hydroxyapatite-based bioceramics. *Acta Biomater.* **2009**, *5*, 743–754.
- (12) Mishra, V. K.; Bhattacharjee, B. N.; Kumar, D.; Rai, S. B.; Parkash, O. Effect of a chelating agent at different pH on the spectroscopic and structural properties of microwave derived hydroxyapatite nanoparticles: a bone mimetic material. *New J. Chem.* **2016**, *40*, 5432–5441.
- (13) Mishra, V. K.; Srivastava, S. K.; Asthana, B. P.; Kumar, D. Structural and Spectroscopic Studies of Hydroxyapatite Nanorods Formed via Microwave-Assisted Synthesis Route. *J. Am. Ceram. Soc.* **2012**, *95*, 2709–2715.
- (14) Sah, M. K.; Rath, S. N. Soluble eggshell membrane: A natural protein to improve the properties of biomaterials used for tissue engineering applications. *Mater. Sci. Eng. C* **2016**, *67*, 807–821.
- (15) Govindaraj, D.; Rajan, M. Synthesis and Spectral Characterization of Novel Nano-Hydroxyapatite from *Moringaoleifera* Leaves. *Mater. Today: Proc.* **2016**, *3*, 2394–2398.
- (16) *Unit Cell Software TJB Holland & SAT Redfern*. 1995.
- (17) Mishra, V. K.; Bhattacharjee, B. N.; Parkash, O.; Kumar, D.; Rai, S. B. Mg-doped hydroxyapatite nanoplates for biomedical applications: A surfactant assisted microwave synthesis and spectroscopic investigations. *J. Alloys Compd.* **2014**, *614*, 283–288.
- (18) Miculescu, F.; Maidaniuc, A.; Miculescu, M.; Dan Batalu, N.; Cătălin Ciocoiu, R.; Voicu, Ș. I.; Stan, G. E.; Thakur, V. K. Synthesis and Characterization of Jellified Composites from Bovine Bone-Derived Hydroxyapatite and Starch as Precursors for Robocasting. *ACS Omega* **2018**, *3*, 1338–1349.
- (19) Miculescu, F.; Maidaniuc, A.; Voicu, S. I.; Thakur, V. K.; Stan, L. T. Progress in hydroxyapatite-starch based sustainable biomaterials for biomedical bone substitution applications. *ACS Sustainable Chem. Eng.* **2017**, *5*, 8491–8512.